Dalton Transactions



PAPER

View Article Online



Cite this: DOI: 10.1039/d0dt01118e

Reversible nickel-metallacycle formation with a phosphinimine-based pincer ligand†

Xiujing Xing, Shaoguang Zhang, Laura M. Thierer, Michael R. Gau, Patrick J. Carroll and Neil C. Tomson *** ***

Pincer ligands have a remarkable ability to impart control over small molecule activation chemistry and catalytic activity; therefore, the design of new pincer ligands and the exploration of their reactivity profiles continues to be a frontier in synthetic inorganic chemistry. In this work, a novel, monoanionic NNN pincer ligand containing two phosphinimine donors was used to create a series of mononuclear Ni complexes. Ligand metallation in the presence of NaOPh yielded a nickel phenoxide complex that was used to form a mononuclear hydride complex on treatment with pinacolborane. Attempts at ligand metallation with NaN (SiMe₃)₂ resulted in the activation of both phosphinimine methyl groups to yield an anionic, *cis*-dialkyl product, in which dissociation of one phosphinimine nitrogen leads to retention of a square planar coordination environment about Ni. Protonolysis of this dialkyl species generated a monoalkyl product that retained the 4-membered metallacycle. The insertion of 2,6-dimethylphenyl isocyanide (xylNC) into this nickel metallacycle, followed by proton transfer, generated a new five-membered nickel metallacycle. Kinetic studies suggested rate-limiting proton transfer (KIE \geq 3.9 \pm 0.5) from the α -methylene unit of the putative iminoacyl intermediate.

Received 24th March 2020, Accepted 20th May 2020 DOI: 10.1039/d0dt01118e

rsc.li/dalton

Introduction

Pincer ligands have attracted interest for their ability to offer both electronic and steric flexibility about a metal center, as needed for rationally tuning the reactivity of metal complexes. Group 10 pincer complexes have been shown to display interesting small molecule activation chemistry and catalytic activity, including C–C cross-coupling chemistry, ketone/aldehyde hydrosilylation and others. Second

A variety of pincer ligands have been applied to Ni chemistry. The PNP scaffold (Chart 1a) studied by Mindiola and coworkers includes two dialkylphosphino groups tethered to a central diarylamido ligand backbone. This combination of a "hard" nitrogen anion with the "soft" phosphine donors creates a ligand framework capable of stabilizing a wide range of oxidation states. (PNP)Ni(I) species were isolable and shown to undergo H–X bond activation (X = H, OH, Bcat, PHPh, and OCH₃) through binuclear oxidative addition. Guan and coworkers isolated a nickel hydride stabilized by a related "hard/"

soft" pincer ligand, PCP (Chart 1a), by treating a (PCP)Ni halide with LiAlH₄. The hydride was shown to serve as an efficient catalyst in the hydrosilylation of ketones and aldehydes.¹³ Hu and co-workers demonstrated that an all-"hard"-donor NNN pincer ligand (Chart 1a) bound to a Ni(II) alkyl complex could cleave the C-X bonds of alkyl halides and afford C-C cross-coupled products.¹⁴ Hu and coworkers also synthesized a Ni(II) hydride by treatment of a (NNN)Ni(II) methoxide complex with diphenylsilane and explored its catalytic reactivity toward hydrodehalogenation of alkyl halides.¹¹

Phosphinimine-based ligands offer a high degree of steric and electronic tunability that may be easily incorporated into pincer frameworks, but these functional groups remain underexplored.²⁵⁻³⁹ The nature of the P-N interaction in the phosphinimine moiety is intriguing in that it is best represented as a zwitterionic bond (Chart 1b). An NBO analysis by Dyson and coworkers found that the dominant resonance structure of phosphazene (HNPH3) involves significant cationic character at P and anionic character at N. 25 This suggests that inclusion of phosphinimine groups in pincer ligands would create a strong donor profile with minimal overall charge when bound to low-valent transition metals. The inclusion of phosphinimine residues on the periphery of a pincer ligand would further offer a tunable and sterically encumbering secondary coordination sphere that can be used to shield the metal center.

P. Roy and Diana T. Vagelos Laboratories, Department of Chemistry, University of Pennsylvania, PA 19104, USA. E-mail: tomson@upenn.edu

[†]Electronic supplementary information (ESI) available: NMR spectra of 1–6 and crystallographic information of 2–5. CCDC 1970109–1970112. For ESI and crystallographic data in CIF or other electronic format see DOI: 10.1039/d0dt01118e

This work: Mononuclear Ni complex

Chart 1 (a) Examples of pincer ligands mentioned in the paper; (b) resonance structures of phosphinimine-based pincer ligand: (c) examples of dinuclear metal complexes with phosphinimine-based ligands reported in literature; (d) target of this work - Mononuclear metal complexes.

The Stephan group has synthesized a series of nickel and palladium complexes with a phosphinimine-based NNN pincer ligand HN(1,2-C₆H₄N=PPh₃)₂. This bis(triphenylphosphinimine) ligand displays adjustable coordination modes, depending on the protonation state of the central amino group. Mononuclear nickel complexes were obtained when the neutral form of the ligand was used, but dinuclear nickel complexes were generated upon deprotonation (Chart 1c). This coordinative flexibility was also demonstrated by Auffrant and coworkers with a 2,6-bis(triphenylphosphiniminomethyl)pyridine ligand.27 Various coordination modes were observed when this ligand was bound to copper, depending on the oxidation state of the metal and the identity of the ancillary ligands (halides, PEt3, MeCN, non-coordinating PF6 anion). For example, this ligand showed a monomeric κ^2 -coordination with Cu(I) halide and dimeric κ^2 -, κ^1 -coordination with Cu(I)PF₆ (Chart 1c). When oxidized to Cu(II), the coordination mode changed to monomeric κ^3 -coordination.

We sought to develop related phosphinimine-containing pincer ligands capable of forming mononuclear metal complexes (Chart 1d). We proposed that decreasing the steric profile of the phosphinimine substituents in the examples described above would favor the formation of mononuclear metal complexes. Herein, we report the synthesis of a methyldiphenylphosphinimine-substituted pincer ligand and its corresponding nickel complexes. This modest change from

Stephan's ligand is shown to impact the nuclearity of the products, providing access to mononuclear Ni complexes supported by an anionic pincer ligand. The resulting organometallic chemistry involving intramolecular C-H activation, insertion chemistry with proton transfer, and the formation of a thermally sensitive nickel hydride are described below.

Results and discussion

Ligand synthesis

 $HN(2-NH_2-C_6H_4)_2$ was treated with chlorodiphenylphosphine in the presence of triethylamine to form a product with phosphinated primary aniline groups, HN[2-NH(PPh₂)-C₆H₄]₂. Alkylation of the phosphino residues with methyl iodide provided the di(phosphonium) intermediate HN[2-NH(PPh2Me)- C_6H_4 ₂[I]₂. Subsequent dehydrohalogenation with a stoichiometric amount of sodium bis(trimethylsilyl)amide generated the target ligand, HN(1,2-C₆H₄N=PPh₂Me)₂ (1), as a lightyellow solid in 67% yield (Scheme 1). This ligand exhibits a ³¹P {1H} resonance at 3.03 ppm in CDCl3, which lies close to that of the PPh3 analog (3.80 ppm).26 The 1H NMR spectrum of 1 shows a characteristic signal at 2.03 ppm for the phosphinimine methyl group (${}^{2}J_{P,H}$ = 12.6 Hz).

Synthesis and characterization of LNiOPh

Metallation of 1 was initially attempted by combining the ligand with NiCl₂(dme) and NaOPh in a 1:1:1 molar ratio in THF to generate LNiCl, but doing so led to a mixture of unidentifiable products by NMR spectroscopy. 40 However, increasing the loading of NaOPh to 2.0 equiv. generated a diamagnetic, red species that gives rise to one 31P{1H} resonance at 34.73 ppm and a doublet at 2.40 ppm (${}^{2}J_{P,H}$ = 13.7 Hz) in the ¹H NMR spectrum for the phosphinimine methyl group. Single crystals of this compound were grown by vapor diffusion of n-pentane into a fluorobenzene solution, and the structure was determined by X-ray crystallography (Fig. 1) to be a distorted square planar nickel(II) phenoxide complex (2), containing an N-deprotonated ligand (Scheme 2). The central amide is closer to the nickel center (1.8467(15) Å) than the phosphinimine nitrogens [1.8975(15) Å and 1.9027(15) Å,

Scheme 1 Synthesis of ligand (1). (i) 2 equiv. PPh2Cl, 15 equiv. NEt3, THF, 23 °C, 12 h; (ii) 2 equiv. Mel, THF, 23 °C, 48 h; (iii) 2 equiv. NaN (SiMe₃)₂, THF, 23 °C, 4 h.

Fig. 1 ORTEP drawings of compound 2 with 50% thermal ellipsoids. H atoms and solvent molecules are omitted for clarity. Left: View perpendicular to the NiN₃O plane. Right: Side-on view along the N3-Ni1 bond. Two of the phosphinimino phenyl groups are converted to wireframe for clarity. 10% Cl disorder on phenoxide was omitted for clarity.

Scheme 2 Synthesis of 2.

Table 1 Selected bond lengths and angles of complex 2

Bond lengths (Å) and angles (°)	2
Ni(1)-O(1)	1.873(3)
Ni(1)-N(1)	1.8975(15)
Ni(1)-N(2)	1.8467(15)
Ni(1)-N(3)	1.9027(15)
P(1)-N(1)	1.6140(16)
O(1)-Ni(1)-N(2)	169.10(11)
N(1)-Ni(1)-N(3)	167.38(7)

Table 1]. These bond lengths are consistent with literature reported square-planar (NNN)NiCl complex,14 with a shorter bond length of Ni-N_{amide} (1.837 Å) and longer Ni-N_{Me2} bonds (1.955 Å). The tendency toward square planar coordination is evident from the N(1)-Ni(1)-N(3) angle of 167.38(7)° and the O(1)-Ni(1)-N(2) angle of 169.10(11)°. Still, the steric pressure about the PhO ligand induced by the Ph2Me-phosphonium residues creates significant warping of the topology of the complex (Fig. 1). This appears to be due to the placement of one aryl group from each phosphinimine in a nearly co-planar arrangement with the phenoxide phenyl ring. Doing so causes significant distortion of the complex from planarity, with the angle between the metal-based (N3NiO) and ligand-based (N_3P_2) planes of 20.1°.

Despite the approximate C_s symmetry displayed crystallographically, the complex exhibits C_{2v} symmetry in solution by NMR spectroscopy, indicating that the complex is able to isomerize the orientation of the phenoxide ligand on the NMR timescale. Given the steric pressure within this system, we find it reasonable to propose that dissociation of a phosphinimine arm may accompany this isomerization process, but more data are needed to support this hypothesis.

Synthesis and characterization of Ni-C-containing metallacycles

The use of phenoxide as both a base and a ligand proved to be a useful strategy for ligand metallation, but we also sought the use of non-nucleophilic bases, which would be expected to provide greater flexibility in the ensuing chemistry. We were interested to find, however, that the outcome of the reaction changed significantly when a stronger base, sodium hexamethyldisilazide (NaHMDS), was used. Treatment of NiCl₂(dme) with 1 equiv. of 1 and an excess (>3 equiv.) of NaHMDS generated a diamagnetic, red species that gave rise to two 31P{1H} NMR signals of equal intensity at 30.2 and 29.9 ppm.

These accompanied four broad peaks in pyr-d₅ in the ¹H NMR spectrum, at 0.65 ppm, 0.30 ppm, 0.05 ppm and -0.17 ppm, that integrated in a ratio of 1:1:1:1. Single crystals of this compound, 3, were obtained from n-pentane/THF. Crystallographic analysis revealed the product to be a dimer in its solid state (Fig. 2, top) wherein two monomers are bridged through two sodium cations. Each monomer contains a square-planar Ni(II) center with two Ni-CH2 groups (Fig. 2, bottom). This product was formed by deprotonation of the methyl groups on the N=PPh₂Me moieties, resulting in the formation of two new Ni-C bonds. One of the phosphinimine N-atoms is dissociated from the Ni center to afford a square planar Ni(II) complex (Scheme 3). The Ni-CH₂ bond lengths of 1.993(2) and 1.9422(18) Å (Table 2) are in the range of other reported Ni-C bond lengths within 4-membered and 7-membered nickel metallacycles, which range from 1.93 Å to 2.15 Å

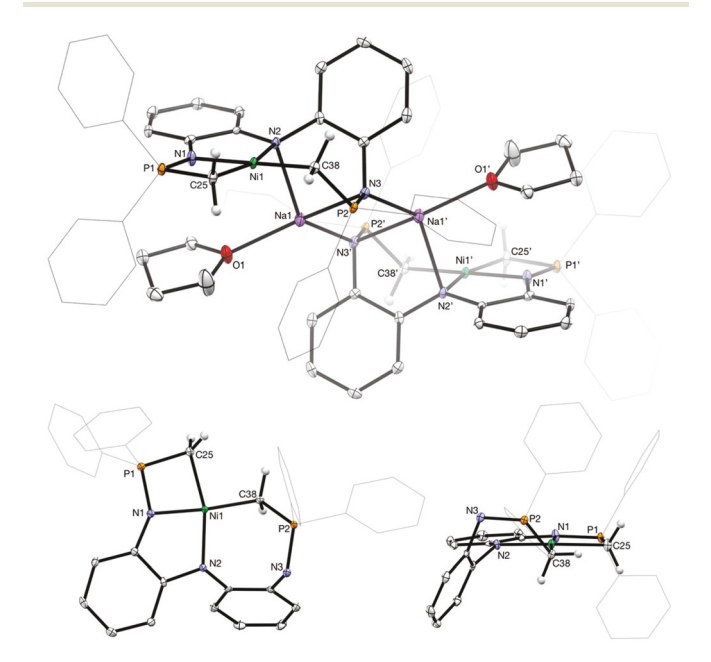


Fig. 2 ORTEP drawings of compound 3 with 50% thermal ellipsoids. Top: Full dimeric structure; H atoms (except those bound to C38 and C25) are omitted for clarity. Bottom left: View perpendicular to the NiC₃₈C₂₅ plane. Bottom right: Side-on view. Two of the phosphinimino phenyl groups are converted to wireframe for clarity.

Scheme 3 Synthesis of 3.

Table 2 Selected bond lengths and angles of complex 3

Bond lengths (Å) and angles (°)	3	
Ni(1)-N(1) Ni(1)-N(2) Ni(1)-C(25) Ni(1)-C(38) P(1)-N(1) P(2)-N(3) C(25)-Ni(1)-N(2)	1.8774(18) 1.9422(18) 1.993(2) 1.950(2) 1.5962(19) 1.6125(18) 163.71(8)	
N(1)-Ni(1)-C(38)	174.73(9)	

and average 1.99 Å;41-57 however, none of these literature examples contain ylidic carbons bound to Ni. The P-C bond length is 1.753(2) Å in the 4-membered ring and 1.761(2) Å in the 7-membered ring, which is shorter than the P-C bond length of the unfunctionalized phosphinimine in 2 (1.7934(19) Å).

In order to determine if 3 exists as a dimer or monomer in solution, DOSY experiments (see ESI, S19-S21†) were performed on 3 and a related mononuclear compound, 4 (see below) in THF- d_8 . The similar diffusion constants of 3 (7.195 \times $10^{-10} \text{ m}^2 \text{ s}^{-1}$) and 4 (6.968 × $10^{-10} \text{ m}^2 \text{ s}^{-1}$) suggest that 3 exists as a monomer in solution. Each of the four broad peaks observed from 0.65 to -0.17 ppm in pyr- d_5 in the ¹H NMR spectrum corresponds to one proton on the CH2 groups, indicating that the protons on the CH2 group are inequivalent. This may be due to Na⁺ association with one face of the molecule, but given the coordinating solvent, we attribute this inequivalence to conformational locking imposed by the fused ring system.

Compound 3 is stable in solution when in the presence of NaHMDS; however, it forms a new diamagnetic species on isolation, as evidenced by the gradual appearance of two ³¹P{¹H} NMR signals of equal intensity at 27.39 ppm and 37.73 ppm in THF- d_8 . The appearance of these features is accompanied by the growth of two doublets in the 1H NMR spectrum, one at 1.72 ppm (${}^2J_{P,H}$ = 12.6 Hz) and the other at -0.92 ppm (${}^2J_{P,H}$ =

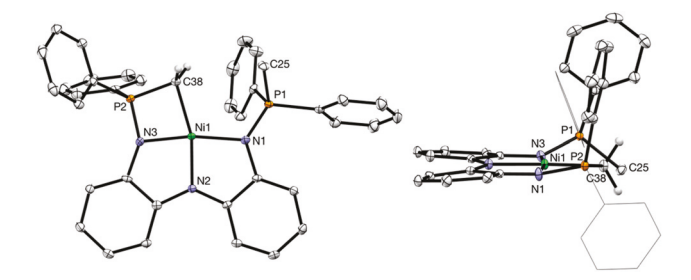


Fig. 3 ORTEP drawings of compound 4 with 50% thermal ellipsoids. H atoms (except those bound to C38) and solvent molecules are omitted for clarity. Left: View perpendicular to the NiN₃C plane. Right: Side-on view. Two of the phosphinimino phenyl groups are converted to wireframe for clarity.

Table 3 Selected bond lengths and angles of complex 4

Bond lengths (Å) and angles (°)	4	
Ni(1)-C(38)	2.0320(19)	
Ni(1)-N(1)	1.9233(17)	
Ni(1)-N(2)	1.8598(16)	
Ni(1)-N(3)	1.8481(17)	
P(1)-N(1)	1.6047(17)	
P(2)-N(3)	1.6020(17)	
C(38)-Ni(1)-N(2)	164.45(8)	
N(1)-Ni(1)-N(3)	170.05(7)	
	()	

4 Hz), that integrated in a ratio of 3:2, respectively. Single crystals of this compound, 4, were obtained from *n*-pentane/fluorobenzene. Crystallographic analysis revealed 4 to result from protonolysis of the 7-membered ring of 3, yielding a product that retained the four-membered metallacycle and reassociated the remaining phosphinimine nitrogen (Fig. 3). The cyclometallated phosphinimine forms a shorter Ni-N distance (1.8481 (17) Å, Table 3) than that of the 4-membered ring in 3 (1.8774 (18) Å). The Ni-CH₂ distance in 4 of 2.0320(19) Å is slightly longer than that of 3. The doublet at -0.92 ppm in the 1 H NMR spectrum is assigned to the Ni-CH₂ protons, based on the relative integration of this signal and its upfield chemical shift. This reaction is reversible and 3 can be obtained by treating 4 with 1.0 equiv. of NaHMDS. Alternatively, 4 can be obtained cleanly in 64% yield by treating NiCl₂(dme) with 1.0 equiv. of 1 and 2 equiv. of NaHMDS (Scheme 4). We find it useful to note that 2 can also be formed from treatment of 4 with 1.0 equiv. of HCl followed by 1.0 equiv. of NaOPh. This reaction may be reversed by addition of 1.0 equiv. of NaHMDS to a solution of 2.

Complex 4 was found to be thermally and photochemically robust. It shows no decomposition as a solid at room temperature under N2 over several months, and heating solutions of 4 at either 80 °C (CD3CN) or 150 °C (C6D5Br) for 72 h did not lead to appreciable decomposition. This complex also shows no decomposition upon irradiation with UV-B light (Rayonet Photochemical Chamber Reactor RMR-400, RPR-3000 Å lamp) over several days.

In addition to its thermal and photochemical stability, complex 4 was also found to be chemically inert toward treat-

Scheme 4 Synthesis of 4.

ment with hydrogen gas, carbon dioxide, and triphenyl silane at 80 °C in C₆D₆. However, 4 was found to react with carbon monoxide to immediately generate an NMR silent species. Recently, the Auffrant group reported the insertion of CO into a phosphinimine-derived Ni-Ph bond to generate a CO inserted product.⁵⁸ Several attempts to isolate the product in our case were unsuccessful; however, treatment of 4 with an aryl isocyanide (isoelectronic to CO) provided a tractable product.

Monitoring the treatment of 4 with 1 equiv. of 2,6-dimethylphenyl isocyanide (xylNC) in C₆D₆ by NMR spectroscopy indicated that 4 was completely consumed within 6 h at 60 °C. Concomitantly, two distinct 31P signals at 43.4 ppm and 35.6 ppm appeared, consistent with the production of a dissymmetric, diamagnetic complex.

Crystallographic analysis revealed a ring-expanded product, 5, in which a tethered vinylamine is C-bound to the metal center (Fig. 4). This product appears to result from both 1,1insertion of the isocyanide into the Ni-C bond and proton migration from the methylene (Scheme 5). A singlet at

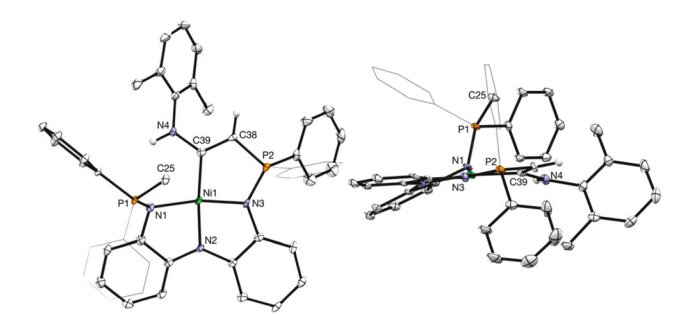


Fig. 4 ORTEP drawings of compound 5 with 50% thermal ellipsoids. H atoms (except those bound to C38 and N4) and solvent molecules are omitted for clarity. Two of the phosphinimino phenyl groups are converted to wireframe for clarity. Left: View perpendicular to the NiN₃C39 plane. Right: Side-on view.

Scheme 5 Synthesis of 5.

Selected P-C coupling constants of complexes in this paper

Compound	$^{1}\!J_{ m P,C}/{ m Hz}$
2	77.8 (CH ₃)
3	78.4 (CH $_2$ in 4-membered ring), 40.9 (CH $_2$ in 7-membered ring)
4	72.1 (CH ₃), 70.1 (CH ₂)
5	76.2 (CH ₃), 164.2 (CH)

6.05 ppm in the product's ¹H NMR spectrum was attributable to the vinyl proton. It is worth noting that the ${}^{1}J_{P,C}$ coupling constant for the cyclometallated =C(H)-P unit (164.2 Hz) is much larger than the one-bond P-C coupling constants for complexes 2, 3 and 4, which range from 40.9 Hz to 78.4 Hz (Table 4). This large ${}^{1}J_{P,C}$ for the methine carbon in 5 reflects the decrease in hybridization at C compared to the sp³-hybridized centers in 2, 3 and 4. The C-C bond in the metallacycle is 1.380(6) Å, indicating partial double bond character. This long C=C distance may result from conjugation with the xylylsubstituted amine $(N_{xyl}-C_{Ni} = 1.381(6) \text{ Å}$, Table 5). We find it interesting to consider that the five-membered metallacycle may also constitute a 6 e⁻ aromatic system comprised of two π -electrons from the metal, two from the vinyl C-C double bond, and two from the phosphinimine double bond. Similar metalloaromaticity has been described for a five-membered Ru-benzoquinonediimine complex,⁵⁹ and such aromatization in the current system may provide a driving force for proton migration. We note, however, that the minimal change in the P-N distance from 4 to 5 may argue against a metalloaromatic system.

Table 5 Selected bond lengths and angles of complex 5

Bond lengths (Å) and angles (°)	5
Ni(1)-N(1)	1.921(4)
Ni(1)-N(2)	1.866(4)
Ni(1)-N(3)	1.865(4)
Ni(1)-C(39)	1.882(4)
C(39)-C(38)	1.380(6)
C(39)-N(4)	1.381(6)
C(38) - P(2)	1.732(4)
C(25)-P(1)	1.797(5)
N(1)-P(1)	1.628(3)
N(3)-P(2)	1.627(4)
C(39)-Ni(1)-N(2)	170.94(16)
N(1)-Ni(1)-N(3)	167.31(16)
N(4)-C(39)-C(38)	120.3(4)
C(39)-C(38)-P(2)	112.5(3)

Scheme 6 Synthesis of 4-d₅.

We were surprised to find that only three proton migration reactions following isocyanide insertions have been reported from across the transition series, 60-62 and two of these were only observable as transient intermediates en route to thermodynamic products. In all cases, double xylNC insertion was observed and no mechanistic data are available.

A deuterium-labelled version of the ligand, $1-d_6$, was formed through the use of iodomethane-d3 during ligand synthesis. Metallation of $1-d_6$ yielded the anticipated perdeuterated product $4-d_5$ (Scheme 6). Monitoring the treatment of $4-d_5$ with 1 equiv. of xylNC in C₆D₆ by NMR spectroscopy indicated that 4- d_5 was completely converted to 5- d_5 within 18 h at 60 °C with two distinct 31P signals at 44.6 ppm and 37.2 ppm appeared (Scheme 7). ¹H NMR spectral data suggested 85% deuterium incorporation into the vinyl moiety, indicating proton migration indeed originates from the Ni-CH₂-L metallacycle backbone.

Reaction rate monitoring by NMR spectroscopy was used to obtain further information about the reaction mechanism. Attempts at generating pseudo-first-order conditions adding an excess (10 equiv.) of xylNC to a THF-d8 solution of 4 resulted in multiple new products as determined by ³¹P{¹H} NMR spectroscopy (ESI, Fig. S67†). Reaction rate monitoring of the conversion of 4 to 5 in the presence of 2.5 equiv. of xylNC generated 5 as the major product over a serviceable timeframe. While these conditions limited the extent of our mechanistic investigation, they provided for observation of reaction intermediates that inform our understanding of the behaviour of

Following addition of 2.5 equiv. of xylNC to a THF- d_8 solution of 4, two peaks appeared concurrently at 41.69 ppm and -8.00 ppm. The ³¹P signal at -8.00 ppm suggests the dissociation of the phosphinimine arm to vacate a site for the isocyanide coordination. These features were assigned to intermediate I, which was found to reach a maximum of 20% conversion at t = 5 min before decaying completely. This decay process proceeded concomitantly with the appearance of two

Scheme 7 Synthesis of 5-d₅

new signals at 29.63 ppm and -7.45 ppm. This new pair of signals was assigned as intermediate II, which was observed to reach 80% conversion at t = 90 min, at which point 5 was observed to form and continued to do so over 6 h until reaching a yield of 80%. Similar results were observed when the reaction was performed with 4-d₅, with ³¹P{¹H} signals at 41.69 ppm and -8.00 ppm (I- d_5) that decayed after 5 min along with the appearance of $II-d_5$ as a broad feature at 29.63 ppm. The product, 5- d_5 , was formed in 80% yield over

Determination of the kinetic isotope effects (KIEs, $k_{\rm H}/k_{\rm D}$) for each step outlined above $(4 \rightarrow I, I \rightarrow II)$ and $II \rightarrow 5)$ were complicated by the rapidity of the transformation $(4 \rightarrow I)$ and the incomplete formation of I and II prior to initiation of the subsequent reaction. However, the reaction profiles for $4 \rightarrow I$ and $I \rightarrow II$ were qualitatively identical between the isotopologues, suggesting that at most these reactions experience a small 2° KIE. A 1° KIE was evident for the conversion of II \rightarrow 5. The incomplete conversion of $I \rightarrow II$ only allows for determination of a minimum KIE for this reaction, but the $k_{\rm H}/k_{\rm D} \ge 3.9$ ± 0.5 clearly implicates a rate-limiting proton transfer for this step.

The chemical structures of intermediates I and II cannot be determined unambiguously based on the available data, but enough data are available to allow for reasonable conjecture. Initial coordination of isocyanide displaces a phosphinimine arm from the metal center to form the square planar intermediate I (Scheme 8). Insertion of the isocyanide into the Ni-C bond via a 1,1-insertion mechanism is the next logical step, but like intermediate I, intermediate II appears to be diamagnetic with two very different chemical environments for the phosphinimine arms. The upfield 31P chemical shifts for each (-8.00 ppm in intermediate I and -7.45 ppm in intermediate II) hew more closely to the chemical shift range of the free ligand than Ni-bound phosphinimines. This suggests either that the insertion product yields an η²-bound iminoacyl intermediate, in which case the functionalized ligand arm would dissociate from the metal in order to avoid formation of a 5.5.3-fused tricyclic system (Scheme 8, pathway 1), or the η^{1} iminoacyl could bind an additional equivalent of isocyanide to retain the square planar coordination geometry (Scheme 8, pathway 2). The former finds support in the structure of 3, which similarly displayed dissociation of a phosphinimine arm in order to facilitate formation of a 7-membered ring. We note that a related metallacyclic η²-iminoacyl has been reported recently.63 The latter proposal is also reasonable, given the affinity of Ni(II) for isocyanides and the apparent ability of isocyanide to displace a phosphinimine arm from Ni. From intermediate II, rate-limiting tautomerization of the imine and reassociation of the phosphinimine nitrogen (with isocyanide dissociation in pathway 2) would then form the final product, 5.

Synthesis and characterization of LNiH

The cyclometallation reactivity described above serves to highlight the rich acid-base chemistry that is available to the phos-

Scheme 8 Proposed mechanism for xylNC insertion.

phinimine residues in the presence of $Ni(\pi)$. The facile interconversion between various states of protonation suggest that these species may serve to mediate proton transfer chemistry in the secondary coordination sphere, and they indicate that the Ni-coordinated phosphinomethylidene moiety exhibits significant nucleophilicity.

While complexes 3 and 4 offer a new direction for use of this ligand system, we close by returning to the generation of mononuclear Ni complexes supported by a tridentate NNN-pincer. In this regard, the phenoxide ligand in 2 proved to be a suitable starting point for introduction of a hydride ligand. The use of HBpin (pin = pinacolate) to form Ni hydrides typically requires long reaction times. ¹⁶ However, the addition of HBpin to 2 in THF quickly generated a dark red diamagnetic compound with the concomitant formation of PhOBPin, as determined by ¹¹B{¹H} NMR analysis of the reaction mixture. A

Scheme 9 Synthesis of 6.

characteristic singlet in the 1 H NMR spectrum of the Ni-containing product at -24.36 ppm is consistent with the formation of the nickel hydride complex **6** (Scheme 9). As with the phenoxide complex, the product presented C_{2v} symmetry in solution by NMR spectroscopy, as indicated by the presence of a 6H doublet resonance at 1.96 ppm ($^{2}J_{P,H}$ = 12.8 Hz) in the 1 H NMR spectrum that corresponded to the two phosphinimine methyl groups and a single 31 P{ 1 H} NMR resonance at 24.5 ppm. When stored in $C_{6}D_{6}$ at room temperature, the product was observed to decompose into free ligand and unidentified species within 24 h, but **6** was found to be stable for longer periods (>7 d) as a solid at -35 °C.

Exposing 6 to carbon monoxide caused rapid decomposition to form free ligand. We propose that CO accelerates N-H reductive elimination to generate 1 and $Ni(CO)_x$ species. Similar acceleration of the decomposition of 6 to form 1 was observed when 6 was treated with PhSiH3. Nickel hydrides have been reported to react with silanes to generate the corresponding nickel silyl species. 10,17 At room temperature, 6 does not react with triphenylsilane or diphenylsilane, but it slowly reacts with phenylsilane. No hydrogen gas was observed, but the formation of diphenylsilane was apparent from NMR spectroscopic monitoring of the reaction mixture. While detailed mechanistic data are not available, this observation is consistent with the notion that interaction of the silane with 6 yields an intermediate from which N-H reductive elimination occurs with greater facility, potentially via a σ -complex that removes electron density from Ni and promotes N-H bond formation. More work is needed to explore the chemistry of the nickel hydride complex 6 and the congeners that may be accessed via related synthetic pathways.

Conclusions

This report describes the development of a mononucleating bis-diphenylmethylphosphinimine-based pincer ligand and its application to the organometallic chemistry of nickel. The use of sodium phenoxide as a base during the metallation of 1 produced a nickel(II) phenoxide complex (2), which ultimately proved to be a competent synthon for a square-planar nickel(II) hydride complex (6) when treated with pinacolborane. Use of an excess of a stronger base, NaHMDS, during the metallation of the ligand resulted in the activation of both phosphinimine methyl groups to form compound 3, which was found to contain both 4- and 7-membered metallacycles. This dialkyl species decomposed to form a mono-protonolysis product that retained the 4-membered metallacycle (4). When treated with

xylNC, this latter product was shown to form a novel five-membered metallacycle (5) that appeared to result from 1,1-insertion and subsequent proton transfer. Further investigation into the reactivity of these complexes is underway.

Experimental section

General considerations

All experiments were carried out under an atmosphere of purified nitrogen using standard Schlenk line techniques or in a dry, oxygen-free glovebox. All glassware, molecular sieves, stir bars, cannulas, and Celite were dried in a 150 °C oven for at least 12 h prior to use. Solvents (tetrahydrofuran, acetonitrile, n-pentane, n-hexane, benzene, fluorobenzene, dichloromethane and diethyl ether) were dried by passage through a column of activated alumina and stored over 4 Å molecular sieves under an inert atmosphere. Deuterated solvents were purchased from Cambridge Isotope Laboratory, dried over Na⁰/benzophenone (THF-d₈, C₆D₆) or CaH₂ (CD₃CN, pyridined₅, and CDCl₃), isolated via vacuum transfer or distillation, and stored under an inert atmosphere over 4 Å sieves. HN(2-NH₂-C₆H₄)₂ was prepared according to the literature procedure.26 Pinacolborane was vacuum transferred and stored at -35 °C prior to use. All other reagents were obtained from commercial sources and used without further purification. ¹H, ¹³C{¹H}, ³¹P{¹H}, ¹¹B{¹H} and 2D NMR (¹H-¹³C HSQC, ¹H-¹H COSY, ¹H-¹³C HMBC, ¹H-³¹P HMBC, ¹H-¹H TOCSY, DOSY) spectra were recorded on Bruker UNI 400, NEO 400, UNI 500 or NEO 600 spectrometers. All chemical shifts (δ) are reported in units of ppm and referenced to the residual protio-solvent resonance for ¹H and ¹³C{¹H} chemical shifts. External H₃PO₄ was used for referencing ³¹P chemical shifts. External BF₃·OEt₂ was used for referencing 11B chemical shifts. Elemental analyses were performed by Midwest Microlab, LLC or on a Costech ECS 4010 analyzer.

Crystallographic data collection and processing

X-ray intensity data were collected on a Bruker D8QUEST⁶⁴ CMOS area detector or on a Bruker APEXII⁶⁴ CCD area detector, employing graphite-monochromated Mo- K_{α} radiation (λ = 0.71073 Å) at a temperature of 100 K. Rotation frames were integrated using SAINT,65 producing a listing of unaveraged F2 and $\sigma(F^2)$ values. The intensity data were corrected for Lorentz and polarization effects and for absorption using SADABS.66 The structure was solved by direct methods by using ShelXT.⁶⁷ Refinement was done by full-matrix least squares based on F^2 using SHELXL-2017⁶⁷ or SHELXL-2018.⁶⁸ All reflections were used during refinement. The weighting scheme used was w = $1/[\sigma^2(F_0^2) + (0.0369P)^2 + 9.9284P]$ where $P = (F_0^2 + 2F_c^2)/3$. Nonhydrogen atoms were refined anisotropically and hydrogen atoms were refined using a riding model.

Synthesis of $HN[2-N(PPh_2Me)-C_6H_4]_2$ (1)

HN(2-NH₂-C₆H₄)₂ (3 g, 15 mmol) was dissolved in THF (100 mL) and cooled to -78 °C. Triethylamine (31 mL,

Chart 2 Numbering scheme used for NMR assignments. Left: Compound 1; right: compound 2.

225 mmol) was added to the stirred solution, followed by dropwise addition of chlorodiphenylphosphine (5.38 mL, 30 mmol). A white precipitate formed immediately. The reaction mixture was warmed to room temperature and stirred for 12 h. The resulting yellow mixture was filtered and volatile materials were removed in vacuo. The crude yellow solid was re-dissolved in THF (100 mL), then methyl iodide (2.1 mL, 37.5 mmol) was added to the stirring solution. The reaction mixture was stirred at room temperature for 12 h. A white precipitate formed during the course of the reaction and was collected by cannula filtration once the reaction was complete. The solid was washed with 3 × 10 mL of THF, dissolved in DCM (150 mL) and cooled to -78 °C. A solution of sodium hexamethyldisilazide (4.13 g, 22.5 mmol) in THF (40 mL) was then added dropwise to the cold solution. The mixture turned light orange within 5 minutes and a white precipitate began to form. The mixture was warmed to room temperature and stirred for 12 h. The white precipitate was removed by filtration and all volatile materials were removed in vacuo to afford 1 as a light-yellow solid. Yield: 6.5 g, 67%. ¹H NMR (500 MHz, CDCl₃, 300 K): δ 8.55 (s, 1H, NH), 7.80 (dd, ${}^{3}J_{P,H}$ = 11.4 Hz, ${}^{3}J_{H,H}$ = 7.9 Hz, 8H, H₈), 7.50 (d, ${}^{3}J_{H,H}$ = 7.6 Hz, 2H, H₃), 7.38 (t, ${}^{3}J_{H,H}$ = 7.3 Hz, 4H, H₁₀), 7.26 (m, 8H, H₉), 6.68 (m, 2H, H₄ or H₅), 6.47 (m, 2H, H₄ or H₅), 6.42 (d, ${}^{3}J_{H,H}$ = 7.5 Hz, 2H, H₆), 2.03 (d, ${}^{2}J_{P,H}$ = 12.6 Hz, 6H, CH_3) ppm. $^{31}P\{^1H\}$ NMR (162 MHz, C_6D_6 , 300 K): δ 3.03 (s, PPh₂Me) ppm. ¹³C{¹H} NMR (101 MHz, C₆D₆, 300 K): δ 139.90 (s, C₂), 138.45 (d, ${}^{2}J_{P,C}$ = 20 Hz, C₁), 132.45 (d, ${}^{1}J_{P,C}$ = 101 Hz, C_7), 131.97 (s, C_{10}), 131.23 (d, ${}^2J_{P,C} = 9.2$ Hz, C_8), 128.46 (d, ${}^{3}J_{P,C}$ = 11.7 Hz, C₉), 119.67 (d, ${}^{3}J_{P,C}$ = 11.5 Hz, C₆), 118.01 (s, C₄ or C₅), 117.45 (s, C₄ or C₅), 113.27 (s, C₃), 14.38 (d, ${}^{1}J_{P,C}$ = 67 Hz, CH_3) ppm. See Chart 2 for hydrogen and carbon numbers assignments. +ESI-MS (m/z): calcd for $[M + H]^{+}$ 596.6, found 596.6.

Synthesis of $[2-N(PPh_2Me)-C_6H_4]_2NNiOPh$ (2)

To a stirred solution of 1 (150 mg, 0.25 mmol) in 20 mL of THF was added NiCl₂(dme) (55.3 mg, 0.25 mmol) and sodium phenoxide (54.4 mg, 0.50 mmol). The color turned from yellow to dark red within 30 min. The red mixture was stirred for 12 h. Volatile materials were removed *in vacuo*, then the crude red residue was washed with 5 mL of hexane and 5 mL of diethyl ether, before extraction with 5 mL of fluorobenzene

and filtration through Celite. Vapor diffusion of *n*-pentane into the filtrate at 23 °C for 48 h afforded 2 as red blocks. Yield: 128 mg, 74%. 1 H NMR (600 MHz, THF- d_{8} , 300 K): δ 7.53 (dd, $^{3}J_{P,H}$ = 12.3 Hz, $^{3}J_{H,H}$ = 7.7 Hz, 8H, H₈), 7.44 (d, $^{3}J_{H,H}$ = 7.9 Hz, 2H, H_{12}), 7.29 (t, ${}^{3}J_{H,H}$ = 7.6 Hz, 4H, H_{10}), 7.21 (m, 8H, H_{9}), 6.98 (d, ${}^{3}J_{H,H}$ = 8.0 Hz, 2H, H₃), 6.46 (m, 2H, H₁₃), 6.28 (m, 2H, H_4), 5.91 (t, ${}^3J_{H,H}$ = 7.2 Hz, 1H, H_{14}), 5.62 (d, ${}^3J_{H,H}$ = 7.7 Hz, 2H, H_6), 5.47 (t, ${}^3J_{H,H}$ = 7.5 Hz, 2H, H_5), 2.40 (d, ${}^2J_{P,H}$ = 13.7 Hz, 6H, CH_3) ppm. ³¹P{¹H} NMR (162 MHz, THF- d_8 , 300 K): δ 34.73 (s, PPh₂Me) ppm. 13 C{ 1 H} NMR (151 MHz, THF- d_8 , 300 K): δ 167.21 (s, C_{11}), 145.94 (d, ${}^{2}J_{P,C}$ = 13.6 Hz, C_{1}), 144.48 (s, C_{2}), 131.88 (d, ${}^{2}J_{P,C}$ = 10.0 Hz, C_{8}), 131.39 (s, C_{10}), 130.13 (d, ${}^{1}J_{P,C}$ = 93.9 Hz, C_7), 128.28 (d, ${}^3J_{P,C}$ = 12.3 Hz, C_9), 127.17 (s, C_{13}), 121.33 (s, C_{12}), 118.44 (s, C_4), 117.76 (d, ${}^3J_{P,C} = 7.5$ Hz, C_6), 113.24 (s, C_3), 112.30 (s, C_{14}), 112.1 (s, C_5), 16.69 (d, ${}^{1}J_{P,C} = 77.8$ Hz, CH₃) ppm. See Chart 2 for hydrogen and carbon numbers assignments. Anal. calcd for C₄₄H₃₉N₃NiOP₂: C, 70.80; H, 5.27; N, 5.63. Found: C, 70.76; H, 5.22; N, 5.59.

Synthesis of $[[2-N(PPh_2CH_2)-C_6H_4]_2Ni]_2Na_2(THF)_2$ (3)

To a stirred solution of 1 (60 mg, 0.1 mmol) in THF (10 mL) was added NiCl₂(dme) (22 mg, 0.1 mmol) and sodium bis(trimethylsilyl)amide (55 mg, 0.3 mmol). The color turned from yellow to red within 5 min. The red mixture was stirred for 12 h, then volatile materials were removed under vacuum. The crude green residue was washed with 5 mL of n-hexane and 5 mL of diethyl ether, then extracted with 5 mL of THF and filtered through Celite. Vapor diffusion of n-pentane into the filtrate at 23 °C for 48 h yielded 3 as red blocks. Yield: 52 mg, 77%. ¹H NMR (500 MHz, Py- d_5 , 300 K): δ 9.05 (br s, 2H, Ar), 8.19 (br s, 2H, Ar), 8.10-7.91 (m, 3H, Ar), 7.70 (br s, 2H, Ar), 7.48-7.30 (m, 9H, Ar), 7.19 (m, 5H, Ar), 6.93 (m, 1H, Ar), 6.81 (m, 2H, Ar), 6.49 (t, ${}^{3}J_{H,H}$ = 7.7 Hz, 1H, Ar), 6.42 (t, ${}^{3}J_{H,H}$ = 7.3 Hz, 1H, Ar), 0.65 (br, 1H, CH₂), 0.30 (br, 1H, CH₂), 0.05 (br, 1H, CH_2), -0.17 (br. 1H, CH_2) ppm. ¹H NMR (400 MHz, THF- d_8) 300 K): δ 8.56 (m, 2H, Ar), 7.93 (m, 2H, Ar), 7.80 (m, 2H, Ar), 7.71-7.60 (m, 2H, Ar), 7.44 (m, 10H, Ar), 7.25 (m, 3H, Ar), 6.85 $(d, {}^{3}J_{H,H} = 8.1 \text{ Hz}, 1H, N-Ph), 6.68 (d, {}^{3}J_{H,H} = 6.5 \text{ Hz}, 1H, N-Ph),$ 6.53 (d, ${}^{3}J_{H,H}$ = 8.0 Hz, 1H, N-Ph), 6.40 (d, ${}^{3}J_{H,H}$ = 7.5 Hz, 1H, N-Ph), 6.35 (t, ${}^{3}J_{H,H}$ = 7.5 Hz, 1H, N-Ph), 6.19 (t, ${}^{3}J_{H,H}$ = 7.6 Hz, 1H, N-Ph), 5.94 (t, ${}^{3}J_{H,H}$ = 7.4 Hz, 1H, N-Ph), 0.22 (dd, ${}^{2}J_{P,H}$ = 12.2 Hz, ${}^{2}J_{H,H}$ = 4.3 Hz, 1H, Ni-C H_{2}), -0.22 (dd, ${}^{2}J_{P,H}$ = 12.1 Hz, $^{2}J_{H,H}$ = 6.8 Hz, 2H, Ni–C H_{2}), -0.46 (d, $^{2}J_{P,H}$ = 11.5 Hz, 1H, Ni– CH_2) ppm. ³¹P{¹H} NMR (162 MHz, THF- d_8 , 300 K): δ 30.23 (s, $PPh_2CH_2Ni)$, 29.92 (s, $PPh_2CH_2Ni)$ ppm. $^{13}C\{^1H\}$ NMR (101 MHz, THF- d_8 , 300 K): δ 154.97 (d, $J_{P,C}$ = 13.6 Hz, Ar), 150.55 (d, $J_{P,C}$ = 6.2 Hz, Ar), 144.79 (d, $J_{P,C}$ = 9.1 Hz, Ar), 141.21 (s, Ar), 141.07 (d, $J_{P,C}$ = 3.7 Hz, Ar), 140.56 (Ar), 139.31 (Ar), 138.20 (Ar), 137.28 (Ar), 136.63 (Ar), 136.14 (Ar), 135.45 (Ar), 132.10 (d, $J_{P,C}$ = 9.7 Hz, Ar), 131.20 (d, $J_{P,C}$ = 10.1 Hz, Ar), 131.11 (d, $J_{P,C}$ = 10.1 Hz, Ar), 130.75 (d, $J_{P,C}$ = 13 Hz, Ar), 130.60 $(d, J_{P,C} = 17 \text{ Hz}, Ar), 130.31 (d, J_{P,C} = 10.8 \text{ Hz}, Ar), 130.04 (d, J_{P,C})$ = 10.5 Hz, Ar), 129.50 (Ar), 128.52 (Ar), 128.44 (d, $J_{\rm P,C}$ = 8.1 Hz, Ar), 128.17 (d, $J_{P,C}$ = 11.0 Hz, Ar), 127.80 (d, $J_{P,C}$ = 10.6 Hz, Ar), 127.12 (d, $J_{P,C}$ = 9.6 Hz, Ar), 123.06 (d, $J_{P,C}$ = 3.0 Hz, Ar), 119.39 $(d, J_{P,C} = 4.0 \text{ Hz}, Ar)$, 118.19 $(d, J_{P,C} = 5.0 \text{ Hz}, Ar)$, 117.19 (s, Ar),

116.15 ($J_{P,C}$ = 3.0 Hz, Ar), 111.74 (s, Ar), 110.51 (s, Ar), -10.29 (dd, ${}^{1}J_{P,C} = 40.9 \text{ Hz}$, ${}^{3}J_{P,C} = 5.4 \text{ Hz}$, Ni– CH_2 in the 7-membered ring), -28.16 (d, ${}^{1}J_{P,C} = 78.4$ Hz, Ni- CH_{2} in the 4-membered ring) ppm. Note: The resonances for P-Cipso carbons were not able to be assigned. Elemental analysis data were not obtained due to the thermal instability of this compound in the absence of added base.

Synthesis of $[2-N(PPh_2CH_2)-C_6H_4]N[2-N(PPh_2Me)-C_6H_4]Ni$ (4)

To a stirred solution of 1 (150 mg, 0.25 mmol) in THF (20 mL) was added NiCl₂(dme) (55.3 mg, 0.25 mmol) and sodium bis (trimethylsilyl)amide (92.4 mg, 0.50 mmol). The color turned from yellow to green within 30 min. The green mixture was stirred for 12 h, then volatile materials were removed under vacuum. The crude green residue was washed with 5 mL of n-hexane and 5 mL of diethyl ether, then extracted with 5 mL of fluorobenzene and filtered through Celite. Vapor diffusion of n-pentane into the filtrate at 23 °C for 48 h yielded 4 as black blocks. Yield: 105 mg, 64%. ¹H NMR (400 MHz, C₆D₅Br, 300 K): δ 8.00 (d, ${}^{3}J_{H,H}$ = 8.2 Hz, 1H, N-Ph), 7.90 (d, ${}^{3}J_{H,H}$ = 7.7 Hz, 1H, N-Ph), 7.80 (m, 8H, Ar), 7.52-7.35 (m, 7H, Ar), 7.20 (br s, 2H, Ar), 7.13 (m, 2H, Ar), 7.03 (m, 3H, Ar), 6.80 (m, 1H, N-Ph), 6.63 (m, 1H, Ar), 6.35 (m, 1H, N-Ph), 6.22 (d, ${}^{3}J_{H,H}$ = 7.7 Hz, 1H, N-Ph), 2.04 (d, ${}^{2}J_{P,H}$ = 12.6 Hz, 3H, CH₃), -0.78 (d, ${}^{2}J_{P,H}$ = 4 Hz, 2H, Ni– CH_2) ppm. $^{31}P\{^1H\}$ NMR (162 MHz, C_6D_5Br , 300 K): δ 27.39 (s, PPh_2Me), 37.83 (s, PPh_2CH_2Ni) ppm. ¹³C{¹H} NMR (101 MHz, C_6D_5Br , 300 K): δ 149.68 (d, J = 13.0 Hz, Ar), 148.27 (d, J = 12.0 Hz, Ar), 145.92 (s, Ar), 144.03 (J = 5.0 Hz, Ar), 134.6 (d, ${}^{1}J_{P,C}$ = 102 Hz, P- C_{Ph}), 132.37 (s, Ar), 132.03 (d, J = 9.9 Hz, Ar, 130.59 (d, J = 10.7 Hz, Ar, 130.20 (d, J = 8.5 Hz,Ar), 128.98 (d, J = 12.2 Hz, Ar), 128.75 (d, J = 11.2 Hz, Ar), 124.99 (s, Ar), 120.66 (s, Ar), 119.48 (s, Ar), 118.72 (d, J = 8.3Hz, Ar), 116.79 (s, Ar), 113.98 (s, Ar), 112.68 (s, Ar), 111.52 (s, Ar), 16.87 (d, ${}^{1}J_{P,C}$ = 72.1 Hz, $PPh_{2}CH_{3}$), -28.57 (d, ${}^{1}J_{P,C}$ = 70.1 Hz, NiCH₂) ppm. Note: The resonance for one type of P-C_{ipso} carbon was not located, presumably due to overlap with the solvent. Anal. calcd for C₃₈H₃₃N₃NiP₂: C, 69.97; H, 5.10; N, 6.44. Found: C, 69.36; H, 4.98; N, 6.28.

Synthesis of [2-C₆H₄-N(PPh₂CH^{xyl}NHC)]NiN[2-N(PPh₂Me)- C_6H_4 (5)

To a stirred solution of 4 (80 mg, 0.12 mmol) in 20 mL of THF was added 2,6-dimethylphenyl isocyanide (16 mg, 0.12 mmol). The reaction mixture was stirred at 60 °C for 6 h, during which time the color turned from green to red. Volatile materials were then removed in vacuo. The red residue was washed with 5 mL of hexane and 5 mL of diethyl ether. The remaining solid was dried under vacuum and collected as a light brown powder. Vapor diffusion of ether into the THF/MeCN solution at 23 °C for 48 h yielded 5 as red blocks. Yield: 86 mg, 90%. ¹H NMR (400 MHz, pyr- d_5 , 300 K): 8.23 (br s, 4H, Ar), 7.70–7.64 (m, 4H, Ar), 7.52-7.26 (m, 14H, Ar), 6.91 (br s, 3H, Ar), 6.84 (m, 2H, Ar), 6.66 (d, ${}^{3}J_{H,H}$ = 7.7 Hz, 1H, Ar), 6.42 (m, 2H, Ar), 6.26 (s, 1H, NHCCH), 6.11 (t, ${}^{3}J_{H,H}$ = 7.5 Hz, 1H, Ar), 3.82 (d, ${}^{2}J_{P,H}$ = 47.5 Hz, 1H, NHCCH), 3.39 (d, ${}^{2}J_{P,H}$ = 13.3 Hz, 3H, PPh₂Me), 2.31 (br s, 3H, ^{xyl}Me), 1.98 (br s, 3H, ^{xyl}Me) ppm. ³¹P{¹H} NMR

(162 MHz, pyr- d_5 , 300 K): δ 42.77 (s, PPh₂CH^{xylNH}CNi), 35.57 (s, *P*Ph₂Me) ppm. 13 C{ 1 H} NMR (101 MHz, pyr- d_5 , 300 K): δ 185.10 $(d_1^2 J_{P.C} = 35.9 \text{ Hz}, \text{NH}CCH), 150.30 (d_1 J_{P.C} = 9.8 \text{ Hz}, \text{Ar}), 149.03$ (s, Ar), 148.91 (s, Ar), 146.96 (d, $J_{P,C}$ = 5.0 Hz, Ar), 145.11 (s, Ar), 138.83 (s, Ar), 135.74 (s, Ar), 134.71 (s, Ar), 132.45 (d, J_{PC} = 9.09 Hz, Ar), 132.40 (d, $J_{P,C}$ = 9.09 Hz, Ar), 131.55 (d, $J_{P,C}$ = 3.0 Hz, Ar), 128.62 (d, $J_{P,C}$ = 11.6 Hz, Ar), 125.90 (s, Ar), 122.71 (s, Ar), 122.08 (s, Ar), 121.58 (d, $J_{P,C}$ = 6.9 Hz, Ar), 117.84 (s, Ar), 115.53 $(d, J_{P,C} = 6.3 \text{ Hz}, Ar), 113.99 (s, Ar), 112.90 (s, Ar), 111.98 (d, J_{P,C} = 6.3 \text{ Hz}, Ar), 113.99 (s, Ar), 112.90 (s, Ar), 111.98 (d, J_{P,C} = 6.3 \text{ Hz}, Ar), 113.99 (s, Ar), 112.90 (s, Ar), 111.98 (d, J_{P,C} = 6.3 \text{ Hz}, Ar), 113.99 (s, Ar), 112.90 (s, Ar), 111.98 (d, J_{P,C} = 6.3 \text{ Hz}, Ar), 113.99 (s, Ar), 112.90 (s, Ar), 111.98 (d, J_{P,C} = 6.3 \text{ Hz}, Ar), 113.99 (s, Ar), 112.90 (s, Ar), 111.98 (d, J_{P,C} = 6.3 \text{ Hz}, Ar), 113.99 (s, Ar), 112.90 (s, Ar), 111.98 (d, J_{P,C} = 6.3 \text{ Hz}, Ar), 113.99 (s, Ar), 112.90 (s, Ar), 111.98 (d, J_{P,C} = 6.3 \text{ Hz}, Ar), 113.99 (s, Ar), 112.90 (s, Ar$ = 3.0 Hz, Ar), 110.66 (s, Ar), 81.98 (d, ${}^{1}J_{P,C}$ = 164.2 Hz, NHCCH), 22.13 (d, ${}^{1}J_{P,C} = 76.2 \text{ Hz}$, PPh₂CH₃), 18.69 (s, xyl-CH₃) ppm. Note: The resonance for two types of P-Cipso carbons were not identified, presumably due to overlap with the solvent. Anal. calcd for C₄₇H₄₂N₄NiP₂: C, 72.05; H, 5.40; N, 7.15. Found: C, 71.89; H, 5.47; N, 7.11.

Synthesis of [2-N(PPh₂Me)-C₆H₄]₂NNiH (6)

To a stirred solution of 2 (30 mg, 0.04 mmol) in 5 mL of THF was added pinacolborane (1 M in THF, 0.04 mL, 0.04 mmol) dropwise at −78 °C. The red solution immediately darkened. The dark red mixture was warmed to room temperature and stirred for 10 min. The product was precipitated by treatment of the crude solution with 10 mL of n-hexane and 10 mL of diethyl ether. The precipitate was extracted with 5 mL of THF, followed by removal of volatile materials in vacuo. A red solid was obtained. Yield: 8 mg, 27%. ¹H NMR (400 MHz, C₆D₆, 300 K): δ 8.08 (d, J = 7.9 Hz, 2H, N-Ph), 7.89-7.67 (m, 2H, N-Ph), 7.58-7.46 (m, 8H, P-Ph_{ortho}), 7.25 (d, ${}^{3}J_{H,H} = 5.7$ Hz, 4H, P-Phpara), 7.11-6.73 (m, 8H, P-Phmeta), 6.34-6.26 (m, 2H, N-Ph), 6.15 (d, ${}^{3}J_{H,H}$ = 8.5 Hz, 2H, N-Ph), 1.96 (d, ${}^{2}J_{P,H}$ = 12.8 Hz, 6H, Me), -24.36 (s, 1H, NiH) ppm. $^{31}P\{^{1}H\}$ NMR (162 MHz, $C_{6}D_{6}$, 300 K): δ 24.5 (s, PPh₂Me) ppm. ¹³C{¹H} NMR and elemental analysis data were not obtained due to the thermal instability of this compound.

Conflicts of interest

There are no conflicts of interest to declare.

Acknowledgements

We thank Dr Jun Gu for useful discussions about 2D NMR spectroscopy. The research was supported in part by the National Institute of General Medical Sciences of the National Institutes of Health under award number R35GM128794. We also thank the Charles E. Kaufman Foundation, a supporting organization of The Pittsburgh Foundation (award number KA2016-85227), and the University of Pennsylvania for financial support. We would like to acknowledge the NSF Major Research Instrumentation Program (CHE-1827457), two NIH supplemental awards (3R01GM118510-03S1 and 3R01GM087605-06S1), and the Vagelos Institute for Energy Science and Technology for supporting the purchase of the

NEO 400 and NEO 600 NMR spectrometers that were used in part of this study.

Notes and references

- 1 J. Choi and Y. Lee, Angew. Chem., Int. Ed., 2019, 58, 6938-
- 2 E. A. LaPierre, M. L. Clapson, W. E. Piers, L. Maron, D. M. Spasyuk and C. Gendy, Inorg. Chem., 2018, 57, 495-506.
- 3 O. V. Ozerov, C. Guo, L. Fan and B. M. Foxman, Organometallics, 2004, 23, 5573-5580.
- 4 F. Schneck, M. Finger, M. Tromp and S. Schneider, Chem. -Eur. J., 2017, 23, 33-37.
- 5 A. I. O. Suarez, V. Lyaskovskyy, J. N. H. Reek, J. I. van der Vlugt and B. de Bruin, Angew. Chem., Int. Ed., 2013, 52, 12510-12529.
- 6 J. I. Van der Vlugt, Chem. Eur. J., 2019, 25, 2651-2662.
- 7 M. Ingleson, H. Fan, M. Pink, J. Tomaszewski and K. G. Caulton, J. Am. Chem. Soc., 2006, 128, 1804-1805.
- 8 J. I. Van der Vlugt and J. N. H. Reek, Angew. Chem., Int. Ed., 2009, 48, 8832-8846.
- 9 D. Adhikari, S. Mossin, F. Basuli, B. R. Dible, M. Chipara, H. Fan, J. C. Huffman, K. Meyer and D. J. Mindiola, Inorg. Chem., 2008, 47, 10479-10490.
- 10 D. Adhikari, M. Pink and D. J. Mindiola, Organometallics, 2009, 28, 2072-2077.
- 11 J. Breitenfeld, R. Scopelliti and X. Hu, Organometallics, 2012, 31, 2128-2136.
- 12 R. Cariou, T. W. Graham and D. W. Stephan, Dalton Trans., 2013, 42, 4237-4239.
- 13 S. Chakraborty, J. A. Krause and H. Guan, Organometallics, 2009, 28, 582-586.
- 14 Z. Csok, O. Vechorkin, S. B. Harkins, R. Scopelliti and X. Hu, J. Am. Chem. Soc., 2008, 130, 8156-8157.
- 15 J. B. Diccianni, J. Katigbak, C. Hu and T. Diao, J. Am. Chem. Soc., 2019, 141, 1788-1796.
- 16 N. A. Eberhardt and H. Guan, Chem. Rev., 2016, 116, 8373-
- 17 J. Hao, B. Vabre and D. Zargarian, J. Am. Chem. Soc., 2015, 137, 15287-15298.
- 18 L. S. Jongbloed, N. Vogt, A. Sandleben, B. de Bruin, A. Klein and J. I. van der Vlugt, Eur. J. Inorg. Chem., 2018, 2018, 2408-2418.
- 19 P. Ren, O. Vechorkin, K. V. Allmen, R. Scopelliti and X. Hu, J. Am. Chem. Soc., 2011, 133, 7084-7095.
- 20 D. Sahoo, C. Yoo and Y. Lee, J. Am. Chem. Soc., 2018, 140, 2179-2185.
- 21 F. Schneck, J. Ahrens, M. Finger, A. C. Stückl, C. Würtele, D. Schwarzer and S. Schneider, Nat. Commun., 2018, 9, 1161.
- 22 F. Schneck, F. Schendzielorz, N. Hatami, M. Finger, C. Würtele and S. Schneider, Angew. Chem., Int. Ed., 2018, 57, 14482-14487.
- 23 Z. Wang, X. Li, H. Sun, O. Fuhr and D. Fenske, Organometallics, 2018, 37, 539-544.

- 24 C. Yoo and Y. Lee, Angew. Chem., Int. Ed., 2017, 56, 9502-9506.
- 25 A. B. Chaplin, J. A. Harrison and P. J. Dyson, *Inorg. Chem.*, 2005, 44, 8407–8417.
- 26 R. Cariou, F. Dahcheh, T. W. Graham and D. W. Stephan, *Dalton Trans.*, 2011, **40**, 4918–4925.
- 27 T. Cheisson and A. Auffrant, *Dalton Trans.*, 2014, 43, 13399–13409.
- 28 S. Al-Benna, M. J. Sarsfield, M. Thornton-Pett, D. L. Ormsby, P. J. Maddox, P. Brès and M. Bochmann, *Dalton Trans.*, 2000, 4247–4257.
- 29 L. P. Spencer, R. Altwer, P. Wei, L. Gelmini, J. Gauld and D. W. Stephan, *Organometallics*, 2003, **22**, 3841–3854.
- 30 R. Bielsa, R. Navarro, T. Soler and E. P. Urriolabeitia, *Dalton Trans.*, 2008, 1203–1214.
- 31 Z.-Y. Chai, C. Zhang and Z.-X. Wang, *Organometallics*, 2008, 27, 1626–1633.
- 32 D. Aguilar, M. Contel, R. Navarro, T. Soler and E. P. Urriolabeitia, *J. Organomet. Chem.*, 2009, **694**, 486–493.
- 33 Z.-Y. Chai and Z.-X. Wang, *Dalton Trans.*, 2009, 8005–8012.
- 34 R. Cariou, T. W. Graham, F. Dahcheh and D. W. Stephan, *Dalton Trans.*, 2011, **40**, 5419–5422.
- 35 M. J. Sgro and D. W. Stephan, *Dalton Trans.*, 2011, 40, 2419-2421.
- 36 R. Cariou, T. W. Graham and D. W. Stephan, *Dalton Trans.*, 2013, 42, 4237–4239.
- 37 T.-P.-A. Cao, G. Nocton, L. Ricard, X. F. Le Goff and A. Auffrant, *Angew. Chem., Int. Ed.*, 2014, 53, 1368–1372.
- 38 J. García-Álvarez, S. E. García-Garrido and V. Cadierno, J. Organomet. Chem., 2014, 751, 792–808.
- 39 I. M. Marín, T. Cheisson, R. Singh-Chauhan, C. Herrero, M. Cordier, C. Clavaguéra, G. Nocton and A. Auffrant, Chem. – Eur. J., 2017, 23, 17940–17953.
- 40 The synthesis of LNiCl has been successful by other methods; the product shows atypical solution-phase behavior that will be reported in due course as part of a broader study on the electronic structure of this species and its analogs.
- 41 (*a*) A. N. Desnoyer, J. Geng, M. W. Drover, B. O. Patrick and J. A. Love, *Chem. Eur. J.*, 2017, 23, 11509–11512;
 (*b*) D. J. Mindiola, R. Waterman, V. M. Iluc, T. R. Cundari and G. L. Hillhouse, *Inorg. Chem.*, 2014, 53, 13227–13238.
- 42 D. S. Dudis and J. P. Fackler, *J. Organomet. Chem.*, 1983, **249**, 289–292.
- 43 D. J. Harrison, A. L. Daniels, I. Korobkov and R. T. Baker, *Organometallics*, 2015, 34, 5683–5686.
- 44 D. J. Brauer, C. Krüger, P. J. Roberts and Y.-H. Tsay, *Chem. Ber.*, 1974, **107**, 3706–3715.

- 45 D. Jin, P. G. Williard, N. Hazari and W. H. Bernskoetter, *Chem. Eur. J.*, 2014, **20**, 3205–3211.
- 46 C. Eaborn, M. S. Hill, P. B. Hitchcock and J. D. Smith, *Chem. Commun.*, 2000, 691–692.
- 47 H. Beurich, R. Blumhofer and H. Vahrenkamp, *Chem. Ber.*, 1982, **115**, 2409–2422.
- 48 M. Faust, A. M. Bryan, A. Mansikkamäki, P. Vasko, M. M. Olmstead, H. M. Tuononen, F. Grandjean, G. J. Long and P. P. Power, *Angew. Chem., Int. Ed.*, 2015, **54**, 12914–12917.
- 49 B. L. Lin, C. R. Clough and G. L. Hillhouse, *J. Am. Chem. Soc.*, 2002, **124**, 2890–2891.
- 50 K. D. Kitiachvili, D. J. Mindiola and G. L. Hillhouse, *J. Am. Chem. Soc.*, 2004, **126**, 10554–10555.
- 51 H. Schmidbaur, A. Mörtl and B. Zimmer-Gasser, *Chem. Ber.*, 1981, **114**, 3161–3164.
- 52 A. M. Mazany and J. P. Fackler, *Organometallics*, 1982, 1, 752-753.
- 53 A. N. Desnoyer, E. G. Bowes, B. O. Patrick and J. A. Love, *J. Am. Chem. Soc.*, 2015, **137**, 12748–12751.
- 54 D. J. Mindiola and G. L. Hillhouse, *J. Am. Chem. Soc.*, 2002, **124**, 9976–9977.
- 55 D. A. Vicic, T. J. Anderson, J. A. Cowan and A. J. Schultz, J. Am. Chem. Soc., 2004, 126, 8132–8133.
- 56 F. W. B. Einstein, K. G. Tyers, A. S. Tracey and D. Sutton, *Inorg. Chem.*, 1986, 25, 1631–1640.
- 57 S. Caddick, F. G. N. Cloke, P. B. Hitchcock and A. K. d. K. Lewis, *Angew. Chem., Int. Ed.*, 2004, 43, 5824– 5827.
- 58 L. Mazaud, M. Tricoire, S. Bourcier, M. Cordier, V. Gandon and A. Auffrant, *Organometallics*, 2020, **39**, 719.
- 59 H. Masui, A. B. P. Lever and E. S. Dodsworth, *Inorg. Chem.*, 1993, 32, 258–267; H. Masui, *Coord. Chem. Rev.*, 2001, 219–221, 957–992.
- 60 T. M. Becker, J. J. Alexander, J. A. Krause, J. L. Nauss and F. C. Wireko, *Organometallics*, 1999, **18**, 5594–5605.
- 61 S. M. Beshourl, P. E. Fanwlck and I. P. Rothwell, *Organometallics*, 1987, **6**, 891–893.
- 62 P. L. Motz, J. J. Alexander and D. M. Ho, *Organometallics*, 1989, **8**, 2589–2601.
- 63 J. W. Nugent, G. Espinosa Martinez, D. L. Gray and A. R. Fout, *Organometallics*, 2017, **36**, 2987–2995.
- 64 APEX3 2016.1-0, Bruker-AXS, Madison, WI, 2016.
- 65 SAINT, 8.38A, Bruker AXS Inc., Madison, WI, 2014.
- 66 L. Krause, R. Herbst-Irmer, G. M. Sheldrick and D. Stalke, J. Appl. Crystallogr., 2015, 48, 3–10.
- 67 F. Neese, Wiley Interdiscip. Rev.: Comput. Mol. Sci., 2012, 2, 73–78.
- 68 G. Sheldrick, Acta Crystallogr., Sect. C: Struct. Chem., 2015, 71, 3–8.